J Comp Physiol B (2015) 185:637–646
DOI 10.1007/s00360-015-0914-8

ORIGINAL PAPER

Functional morphology of the respiratory organs in the cellar spider *Pholcus phalangioides* (Arachnida, Araneae, Pholcidae)

Anke Schmitz[1]

Received: 18 December 2014 / Revised: 20 May 2015 / Accepted: 22 May 2015 / Published online: 29 May 2015

Abstract Morphometric evaluation of the lungs of male and female cellar spiders (*Pholcus phalangioideus*) was carried out in 2 test groups with different body masses (mean value 10.8, males, and 26.6 mg, females). Males have significant higher lung volume to body mass ratios (2.49 vs. 2.13 × 10^{-3} cm^3 g^{-1}), which might result from the differences in body mass between sexes. Moreover, males have slightly more respiratory surface area per body mass (8.2 vs. 7.7 cm^2 g^{-1}) and a little bit larger morphological diffusing capacities for oxygen (9.3 vs. 8.2 nmol s^{-1} g^{-1} kPa^{-1}) than females, but both values were not significant. Metabolic rates were measured using flow through respirometry under video tracking: the CO_2 release of male and female spiders was measured. Resting rates were 1.7 (males) and 1.5 nmol s^{-1} g^{-1} (females). Gluing of one spiracle did not influence the resting metabolic rate. Factorial scopes during stimulation to maximum metabolic rates were about 12 in intact animals, while elimination of one spiracle reduced the factorial scope to 5.2. Comparison with other araneomorph spiders strengthens the hypothesis that tracheae in spiders increase the metabolic rates of the tracheated species and do not only replace reduced lung capacity.

Keywords Respiratory system · Lungs · Stereology · Respirometry

Communicated by G. Heldmaier.

✉ Anke Schmitz
ankeschmitz@uni-bonn.de

[1] Institute for Zoology, Rheinische Friedrich-Wilhelms-University Bonn, Poppelsdorfer Schloss, 53115 Bonn, Germany

Introduction

Pholcus (Araneae, Araneomorphae, Pholcidae) is a cosmopolitan spider genus. The genus can be found in Asia, Africa, America, Australia and in Europe. In mid-Europe, *P. phalangioides* lives almost exclusively in buildings. This species has very long legs and a pale skin colour.

Araneomorph spiders are the only animal group in which lungs and tracheae collaborate (Foelix 1992), while Mygalomorphae breathe exclusively with lungs. In literature, some work exists that deals with this collaboration (Anderson 1970; Opell 1987; Prestwich 1983b; Schmitz 2004, 2005, 2013; Schmitz and Perry 2001, 2002). While in most spiders tracheae are of low importance (Schmitz 2005; Schmitz and Perry 2002), in some families, evaluated in Salticidae, they make more than 25 % of the entire diffusing capacity of the respiratory organs (Schmitz and Perry 2001). In some families, tracheae became the dominant respiratory organ. This is the case, e.g., in Dysderidae and Segestriidae. As it was shown in Salticidae (Schmitz 2005), also in other spider families tracheae take over special task for separate functions. In the Uloboridae, tracheae deliver O_2 to the leg muscles and supply, therefore, web constructing (Opell 1987). In Salticidae, tracheae support the aerobic metabolism only at the most intense physical exercise. At low and medium activity, tracheae may play their main role in the local supply of O_2 to organs that are not involved in running activity (Schmitz 2005). Moreover, previous studies are consistent with the hypothesis that tracheated spiders have greater aerobic capabilities during exercise (Anderson 1970; Levi 1976; Prestwich 1983b; Schmitz 2004). In Pholcidae, no tracheae are available (Paul et al. 1994; Strazny and Perry 1987). The second lung pair disappeared as in many other spider families, but was not replaced by tracheae.

With the present paper, we tested the hypothesis that members of the Pholcidae have a lower aerobic metabolism than wolf and jumping spiders and that the lungs have about the same diffusing capacity for oxygen. This would be another evidence that tracheae in spiders are additional respiratory structures that are normally used for special metabolic demands.

Materials and methods

Experimental animals for morphological investigations and tissue processing

Two groups with 6 animals of *P. phalangioides* were investigated (Table 1). All animals were caught in the vicinity of Bonn and maintained in plastic boxes until further processing. Water was always available and spiders were fed *Drosophila* every other day. The animals were cold-anaesthetized, weighed, and the opisthosoma was cut off. The opisthosomae were immersed immediately in cold glutaraldehyde in cacodylate buffer (pH 7.1, 390 mOsmol l^{-1}, 4 °C). The samples were fixed overnight, washed in buffer and postfixed in 1.5 % OsO_4 in the same buffer for 2 h at 4 °C. The samples were then dehydrated through an ethanol series and embedded in Epon 812. Semithin Sections (0.5 µm) and ultrathin sections were made with a Diatome diamond knife. Semithin sections were stained with toluidin blue/borax solution while the ultrathin sections were contrasted with uranyl actetate and lead citrate. Sections were evaluated using a Zeiss EM 109.

Volume determination: Cavalieri principle on vertical sections

The volumes of the lungs were determined using the Cavalieri principle (Michel and Cruz-Orive 1988) combined with the vertical section method (Baddeley et al. 1986). The Cavalieri principle estimates volumes as the total cross-sectional area multiplied by the distance between the sections. For each animal, we took 10 equidistant semithin sections of each lung (Fig. 1). For the volume determination, we used a light microscope (Leitz Dialux 20) with a drawing tube, and a light box on which we placed the test array (Perry et al. 1994). The volumes of the lungs (tissue and lumen) were evaluated by point-counting at final magnification of 750×. Volumes of tissue and lumen of the lungs were determined on electron micrographs at a final magnification of 3350×, with the test grid placed directly onto the micrographs.

Surface areas and barrier thickness: vertical sections

The surface areas of the lungs were determined on semithin sections using 60 symmetrically distributed fields per animal. The areas of the inner surfaces (S_i) and the outer

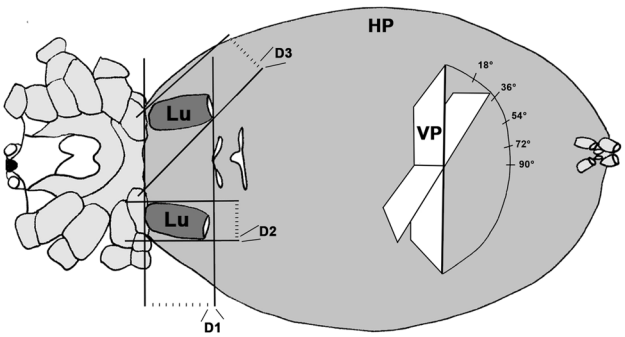

Fig. 1 Schematic drawing of the pro- and opisthosoma of *P. phalangioides* showing the lungs (lu) and a demonstration of the sampling methods for combined Cavalieri principle and the vertical section method. The *horizontal plane* (HP) is the frontal plane of the spider. The planes of section, *vertical planes* (VP) are in the *vertical axis*, perpendicular to HP. The lungs were cut into 10 pieces of equal thickness, the planar walls of which are separated by distance *D*. The location of the first (starting) section was chosen at random within an interval of *D*. In each group, animals were rotated sequentially about the axis of the *vertical planes*, according to the systematic random sampling method (Gundersen and Jensen 1987). We started at a randomly chosen angle within 0–18° from the original orientation (the transverse axis is 0!) for the first animal and added 18° for each further animal. Three examples are given at theoretical angles of 0, 45 and 90° (*D*1, *D*3, *D*2)

Table 1 Body masses and stereological data for the lungs

Test group (mean body mass)	Lung volume ($\times 10^{-6}$ cm^3)	Lung volume/body mass ($\times 10^{-6}$ cm^3 mg^{-1})	CV (%)	CE (%)	Biological variance (%)	ANOVA *P*
Males (10.8 mg, ±0.55, range 9.9–11.5 mg, $N = 6$)	26.8	2.5	9.6	3.9	8.8	
Females (26.6 mg, ±0.58, range 25.9–27.2 mg, $N = 6$)	57.2	2.13	10.3	4.2	9.4	<0.05

CV coefficient of variation, *CE* coefficient of error, *ANOVA* for lung volumes/body mass

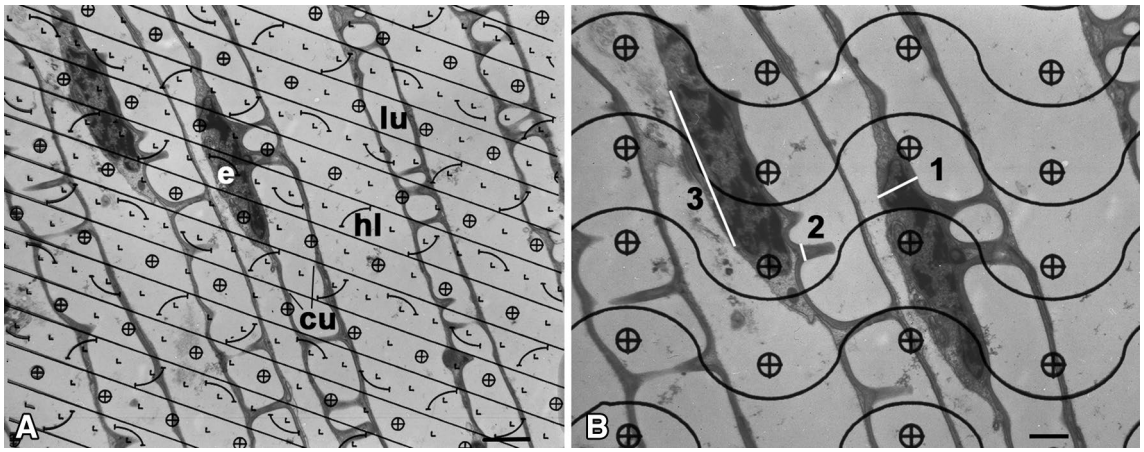

Fig. 2 Electron micrographs of the lungs to show the principles of sampling methods for surface-to-volume ratio measurements S_V (**a**) and barrier thickness measurements (**b**). The corresponding test arrays are superimposed. For S_V, the intersections of the test lines (*cycloid arcs*) with the surface are counted. For the measurements of the barrier thickness, the starting points were selected in an unbiased way using the intersections of the test lines with the surface (**b**). Respiratory surfaces (S_R) are defined as those surfaces exposed to respiratory medium that are not connected by a measuring line to another such surface. In **b** *line 1* (S_R) gives an example for measurement lines that connect the inner with the outer surface of the lungs, *line 2* connects 2 points at the inner surface and *line 3* connects 2 points at the outer surface. *c* cuticle, *e* epidermis, *hl* hemolymph, *lu* air-filled lumen. *Scale bar* is 2 µm in (**a**) and 1 µm in (**b**)

surfaces (S_o) and the surfaces of the border between the cuticle and the epidermis (S_{c-e}) were determined from their respective surface-area-to-volume ratios (S_V) multiplied by the volume of the lungs (tissue and lumen). The S_V of each component was determined by point- and intersection counting at a final magnification of 1600× (Fig. 2a). S_V was calculated as $S_V = 2I/L$, where I is the number of intersections of the test line with the surface and L is the total length of test lines covering tissue and lumen of the lungs. Respiratory surface areas (S_R) were evaluated during measurements of barrier thickness (Fig. 2b). Data were pooled and evaluated for the 2 groups of animals (Howard and Reed 1998).

The barrier thickness of epidermal and cuticular layers was measured from transmission electron micrographs using the stereomicroscope and a half-logarithmic ruler in randomly chosen directions at the final magnification of 14,500× (Fig. 2b) (Perry 1981). The harmonic mean lengths (l_h) of the measured distances (l_i) were calculated and were then converted to the harmonic mean barrier thicknesses as $\tau = (2/3)l_h$ (Weibel and Knight 1964). According to Fick's first law, thin regions are more relevant for gas exchange than thick regions, so the harmonic mean, which weights in favour of small values, is more relevant than the arithmetic mean. In the mathematical derivation for the determination from randomly oriented sections, the harmonic mean of measured lengths must be multiplied by the factor 2/3 to compensate for an overestimate due to the random orientation of the measured intercepts (Weibel and Knight 1964).

Anatomical diffusion factor and diffusing capacity

The anatomical diffusion factors (ADFs) (Perry 1978) were calculated as the respiratory surface area (S_R) in relation to body mass (S_R/M_B) divided by the harmonic mean barrier thickness (τ) of the respective layers. For the inner surface (leading from the air to the hemolymph), we used the inner respiratory surface area for the ADF of the cuticle and the surface area of the border between the cuticle and epidermis for the ADF of the epidermis. For the outer surface (leading from the hemolymph to the air), we used the outer respiratory surface area for the ADF of the epidermis and the surface area of the border between the cuticle and the epidermis for the ADF of the cuticle.

The morphological oxygen diffusing capacities (D_{O_2}) were calculated for each of the 2 layers as the product of the ADFs and Krogh's diffusion coefficient (K_{O_2}), corrected to 20 °C (Bartels 1971; Krogh 1919). For epidermis, we used the corrected, published value for rat lung tissue ($K_{O_2} = 2.05 \times 10^{-7}$ cm^2 min^{-1} kPa^{-1}) and for cuticle that for chitin (1.28×10^{-7} cm^2 min^{-1} kPa^{-1}). Since Krogh's diffusion coefficient for carbon dioxide (K_{CO_2}) in chitin or in arthropod epidermis is assumed to be about 35 times greater than K_{O_2} in the same tissue (Bartels 1971; Krogh 1919), we used this value to estimate the morphological carbon dioxide diffusing capacity (D_{CO_2}). For chitin, this value might be too high. But for comparison with other species (see "Discussion"), it is necessary to use the same values as in the relevant papers (Schmitz and Perry 2001, 2002). The total oxygen and carbon dioxide diffusing capacity (D) of the walls

of the lungs was calculated as the reciprocal of the sum of the reciprocal values of the diffusing capacities of cuticle (D_c) and epidermis (D_e), respectively (Weibel 1970/1971): $D = 1/(1/D_c + 1/D_e)$.

Respirometry

An open-flow system was used to measure rates of CO_2 release during rest and activity. A 20-ml plexiglas container with a rough bottom was used as an animal chamber. The temperature in the chamber and in the air stream was held constant at 20 °C by a water bath. Outside air was pumped into the chamber with a flow rate of 80 ml min^{-1}, adjusted by an Aalborg flow meter. The air initially passed through a soda lime scrubbing column and a series of containers filled with NaOH to remove both CO_2 and water. The air was then rehydrated by a saturated NaCl solution to 30.5 % relative humidity passed through the reference chamber of the gas analyzer and the animal chamber and was finally drawn into the CO_2 analyzer (URAS 14, ABB). The CO_2 analyzer interfaced with a PC for data acquisition. V_{CO_2}/t was calculated from fractional concentrations of CO_2 entering (FI) and leaving (FE) the animal chamber using the equation: $V_{CO_2}/t = \left(FE_{CO_2} - FI_{CO_2}\right) \times$ flow rate (Withers 1977), where flow rate is 80 ml min^{-1} and FI is zero. The rate of CO_2 release was converted to volume of CO_2 per unit time and gram tissue (nmol s^{-1} g^{-1}) at STPD. A CCD video camera was placed above the animal chamber and animal behaviour was recorded during measuring periods using a PC video capture card. Animals were weighed before and after each set of experiments, with the actual mass during a single experiment assuming a linear mass decrease over time.

Experiments were carried out in which we measured metabolic rates during rest, during alertness between activity periods, during spontaneous activity and during forced activity. In the first set of experiments, animals were allowed to habituate to the experimental chamber for 2 h. Afterwards, metabolic rates were measured under artificial light and under video tracking for different time periods during which resting phases and spontaneous activity phases occurred. Overnight, animals were habituated to darkness. During the following measuring period, only infrared illumination supported the function of the video camera.

Phases of rest and activity occurred. Animals were defined to be in rest phase when they were motionless for at least 30 min.

In a second set of experiments, animals were forced to the greatest possible metabolic rates; this was done under visible light and video tracking. Animals were motivated by shaking of the experimental chamber with the support of small bouncing plastic beads. Spiders struggled with the beads or tried to escape, thus activity was not a constant running at maximum speed. This activity, however, should cause maximum metabolic rates as the highest metabolic rates may occur when spiders are engaged in less than maximum activities that require low prosomal hemolymph pressures and thus permit constant circulation and gas exchange (Prestwich 1983b). An individual spider was stimulated for 120 s. None of the animals could be stimulated for longer than this time period and some animals stopped moving before the end of 120 s. The speed of the activity could not be quantified in these experiments, but was assumed to be 8 cm s^{-1} for the figures. This value was chosen arbitrarily to make the results clearly visible in the figures. Males were more aggressive and thus easier to stimulate locomotion than females. Only those experiments in which animals were highly active for the entire 120 s (±5 s) were evaluated. Factorial scopes were calculated from the individual resting rate of a spider and the individual maximum CO_2 release. Differences among sexes were evaluated using ANOVA statistics. To examine the influence of body mass, differences in intraspecific resting rates were additionally tested using ANCOVA statistics (Packard and Boardman 1988).

To avoid mistakes in V_{CO_2}/t due to the location of the spider relative to the output opening, connection tubes were kept as short as possible. Additionally, the experimental chamber was cube shaped and a high flow rate (80 ml min^{-1}) was chosen. The movement of the plastic beads in the stimulation experiments was assumed to stir the air in the chamber. Time lags of 10–14 s between the experimental chamber and the CO_2 analyzer were calculated and all times given in the results and in the figures were corrected for these values. This was possible as the activity of the animals was continuous for the 2 min and, therefore, a steady state trace resulted.

Statistics

To evaluate the estimator variance, we calculated the standard deviation (SD) and coefficient of error (CE) of our barrier thickness measurements. Because τ is calculated from the harmonic mean of the intercept lengths and SD for the harmonic mean is not defined, we calculated SD and CE of the arithmetic mean of the intercept lengths (measured line lengths) (Table 2). As S_V was evaluated on single fields, we calculated the estimator variance of S_V as the SD and CE of the values for each field (Table 2).

For the Cavalieri principle, the precision of the estimate (total variance of the counted points, or var P) depends on the noise (inaccuracy of the test array) and the variance of the sum of the areas $\left(\text{var}\sum_{\text{area}}\right)$: $\text{var}P = \text{noise} + \text{var}\sum_{\text{area}}$ (Gundersen and Jensen 1987; Howard and Reed 1998). The coefficient of error is calculated from var$P$

Table 2 Diffusion barrier τ and for surface-area-to-volume ratios (S_V)

	Test group	τ (μm)	Arithmetic mean of l_i (μm) ± SD	CE (%)	Number of measurements	ANOVA P
Cuticle	Males	0.08	0.21 ± 0.22	3.5	1037	
	Females	0.085	0.19 ± 0.16	2.6	1091	0.16
Epidermis	Males	0.08	0.27 ± 0.38	4.3	1037	
	Females	0.087	0.30 ± 0.39	3.9	1091	0.10
	Test group		Arithmetic mean (cm^{-1}) ± SD		Number of fields evaluated	
Inner surface (cuticle)	Males		4014 ± 1815	2.5	327	
	Females		4200 ± 2175	2.9	306	0.58
Outer surface (epidermis)	Males		3867 ± 1800	2.6	327	
	Females		4080 ± 2195	3.1	306	0.57
Surface between cuticle and epidermis	Males		3378 ± 1578	3.0	327	
	Females		3599 ± 1643	2.7	306	0.5

Descriptive statistics for measured line lengths l_i and S_V are given

and the sum of all counted points according to: CE $\left(\sum P\right) = \sqrt{\text{var}P}/\sum P$ (Cruz-Orive 1993; Howard and Reed 1998). To test the biological variance (interindividual variation) in our test groups, we used the volumes of the lungs per body mass, as these measurements are independent of the cutting angle. We calculated CV according to: $CV^2 = \text{obsCV}^2 - CE^2$, where obsCV is the observed coefficient of variation and CE is the coefficient of error of the measurements (Howard and Reed 1998).

For comparison between the test groups, we carried out ANOVA statistics.

Results

Volumetry and barrier-thickness

The lung volume per body mass in males is slightly higher in females (Table 1). The inter-individual variation of volumes (biological variance) is about 9 % in both sexes. Barrier thickness (τ) is less than 0.1 μm for both cuticular and epidermal layers in males and females (Table 2). This gives a total diffusion barrier of 0.165 μm for males and 0.167 μm for females.

Surface-area-to-volume ratios, surface areas, the anatomical diffusing factors and the diffusing capacities

Surface-area-to-volume ratios (S_V) are given in Table 2. All values are slightly smaller in males but without any difference using ANOVA.

Surface areas, respiratory surface areas and respiratory surfaces/M_B together with the statistics are given in Table 3. Because of the mass of the animals, lung surfaces show differences between the sexes. But looking at the surfaces/M_B, differences no longer exist. The outer and inner respiratory surface areas are smaller than the total outer and inner surface areas. This is because of the enlargement of the surface area by the epidermis, the taenidia and the cuticular struts (Fig. 2). ADFs for the outer and inner respiratory surfaces per body mass, separated from epidermis and cuticle, are given in Table 3. They show the differences between sexes ($P < 0.05$). Calculated diffusing capacities for oxygen were 9.3 nmol s^{-1} g^{-1} kPa^{-1} for males and 8.2 nmol s^{-1} g^{-1} kPa^{-1} for females. For carbon dioxide, values were 349.7 nmol s^{-1} g^{-1} $kPa^{-1}$for males and 283.2 nmol s^{-1} g^{-1} kPa^{-1} for females. This value might be too high for CO_2 passing through chitin, but unfortunately for this procedure no published values exist. Males thus have slightly higher diffusing capacities for both gases.

Respirometry

Both males and females showed no clear diurnal rhythm regarding activity and respiration. In addition, resting values did not differ in complete darkness and under infrared light. Therefore, mean values were calculated from both conditions. The room, in which experiments were carried out, was not completely silent because of gas-transporting pumps and the air-conditioning system. Even if these machines were extremely silent, it cannot be excluded that they caused some disturbances. Therefore, the real basal metabolic rates could be even lower than the measured values. But as the natural environment of the animals is also not completely silent, the acoustic disturbance was considered tolerable. Females had a lower mass-specific resting rate than males (Table 4). This was confirmed by ANCOVA ($F = 6.7$; $P = 0.012$). Females with one spiracle glued had

Table 3 Surface areas (cm^2) and anatomical diffusing factors (ADF, $cm\ g^{-1}$) per body mass for inner and outer respiratory surfaces

Test group	Inner surface area, S_i ($\times 10^{-3}$ cm^2)	Inner respiratory surface area ($\times 10^{-3}$ cm^2)	Inner respiratory surface area/body mass ($cm^2\ g^{-1}$)	Surface area between cuticle and epidermis ($\times 10^{-3}$ cm^2)	Outer surface area, S_o ($\times 10^{-3}$ cm^2)	Outer respiratory surface area ($\times 10^{-3}$ cm^2)	Outer respiratory surface area/body mass ($cm^2\ g^{-1}$)
Males	107.4	88.3	8.2	90.4	103.4	92.5	8.6
Females	240.3	204.6	7.7	205.9	233.5	207.3	7.8
ANOVA *P*	<0.001	<0.001	0.16	<0.001	<0.001	<0.001	0.17

Test group	ADF		
	Inner surface cuticle ($\times 10^3$ $cm\ g^{-1}$)	Inner surface epidermis ($\times 10^3$ $cm\ g^{-1}$)	Outer surface cuticle ($\times 10^3$ $cm\ g^{-1}$)	Outer surface epidermis ($\times 10^3$ $cm\ g^{-1}$)
---	---	---	---	---
Males	1022	1084	1110	1046
Females	904	889	895	910
ANOVA *P*	0.045	0.038	0.04	0.043

not a different resting rate compared with intact females (Table 4).

Above resting rates, CO_2 release included phases of motionless alertness and spontaneous activities. As spiders have long legs and the experimental chamber is small for these legs, animals were not able to walk, but tried to do so. If the experimenter entered the experimental room, all animals responded by a slight increase in CO_2 release. This alertness increased the metabolic rate only slightly (2.6–3.0 times resting rate). Spontaneous movements, however, caused a factorial scope of up to 3.6 (males) or 3.9 (females). While the metabolic rate during these phases was not different between males and females, females with one glued spiracle had a significant lower value for the highest spontaneous activity (Table 4).

Stimulation to maximal activity resulted in individual variations and, therefore, a high standard deviation (Table 4). CO_2 release was burst like and the maximum CO_2 value lasted only a few seconds (Fig. 3). The start of stimulation always caused a short decrease in CO_2 release in females, while this was unusual in males (Fig. 3). The maximum CO_2 release was slightly higher in males than in females and about twice as much between intact and restricted females. Animals were active after the 120-s stimulation or alert, but normally did not reduce their metabolic rates to resting rates (Fig. 3). Therefore, the time between maximum CO_2 release and resting rate is not only a function of metabolism alone but also a function of stress caused by attention. Thus, the recovery time was calculated as half-time recovery. This was defined as the time between end of stimulation and return to half of the maximum CO_2 release (Table 4). Restricted females had the longest half-time recovery while male had the shortest. After stimulation, restricted females had the greatest surplus amount of CO_2 per time (Table 4). Time between end of stimulation and maximum CO_2 release was smallest in restricted females and biggest in males. In females, the maximum CO_2 release was often reached during stimulation time (Fig. 3b, c).

Discussion

Between species, life-styles and life spans, body masses and behaviour could result in differing metabolic rates (Foelix 1992). Also temperature has an influence on the metabolic rate (Schmalhofer 2011) but this is not relevant for the present study as the spiders were measured all at the same temperature. In other spider species, factorial scopes during locomotory activity are between 2 and 12, in Lycosidae sometimes even up to 22 for short periods (Anderson 1970; Culik and McQueen 1985; Ford 1977a, b; Humphreys 1977; Kotiaho 1998; McQueen 1980, 1981;

Table 4 CO_2 release during rest, spontaneous and forced activity and data for half-time recovery after forced activity

	P. phalangioides Males	*P. phalangioides* Females	*P. phalangioides* Females 1 spiracle glued
Body mass (mg)	11.3 ± 0.6, range 10.6–12.9 $N = 12$	27.6 ± 0.8, range 26.5–29.4 $N = 27$	28.3 ± 0.7, range 27.3–29.6 $N = 14$
Rest (nmol s^{-1} g^{-1})	1.72 ± 0.19 $n = 33$	1.48 ± 0.32^{+} $n = 59$	1.6 ± 0.3 $n = 30$
Alertness and spontaneous activity (nmol s^{-1} g^{-1})	4.45–6.17 $n = 30$	3.98–5.76 $n = 45$	3.88–4.2$^{\#}$ $n = 14$
Factorial scope	2.6–3.6	2.7–3.9	2.4–2.8
Maximum CO_2 release during forced activity (120 s) (nmol s^{-1} g^{-1})	19.81 ± 3.7 $n = 36$	17.71 ± 3.7* $n = 46$	9.0 ± 2.8$^{\#}$ $n = 26$
Factorial scope	11.52	11.97	5.2
Time of activity: 120 s			
Time to half-recovery (s)	102.5 ± 40.9 $n = 36$	138.7 ± 76.3 $n = 46$	398 ± 224.4$^{\#\#}$ $n = 26$
CO_2 at half-recovery (nmol g^{-1})	1385.1 ± 226.4	1748.7 ± 654.2*	2322.9 ± 781.0$^{\#}$
CO_2 at half-recovery (nmol s^{-1} g^{-1})	14.58 ± 3.1	13.83 ± 3.83	6.64 ± 2.1$^{\#\#}$
Time between end of stimulation and CO_{2max} (s)	14.0 ± 29.5	6.43 ± 24.7**	3.5 ± 32.23$^{\#\#}$

Values are mean ± SD. Differences were tested with ANOVA and ANCOVA

Significant differences by ANCOVA are marked by a plus $^{+}$ and by ANOVA by asterisks (* $P < 0.01$, ** $P < 0.001$) for comparisons between males and females and by hatch marks ($^{\#}$ $P < 0.01$, $^{\#\#}$ $P < 0.001$) for comparison of intact females and females with one lung spiracle sealed

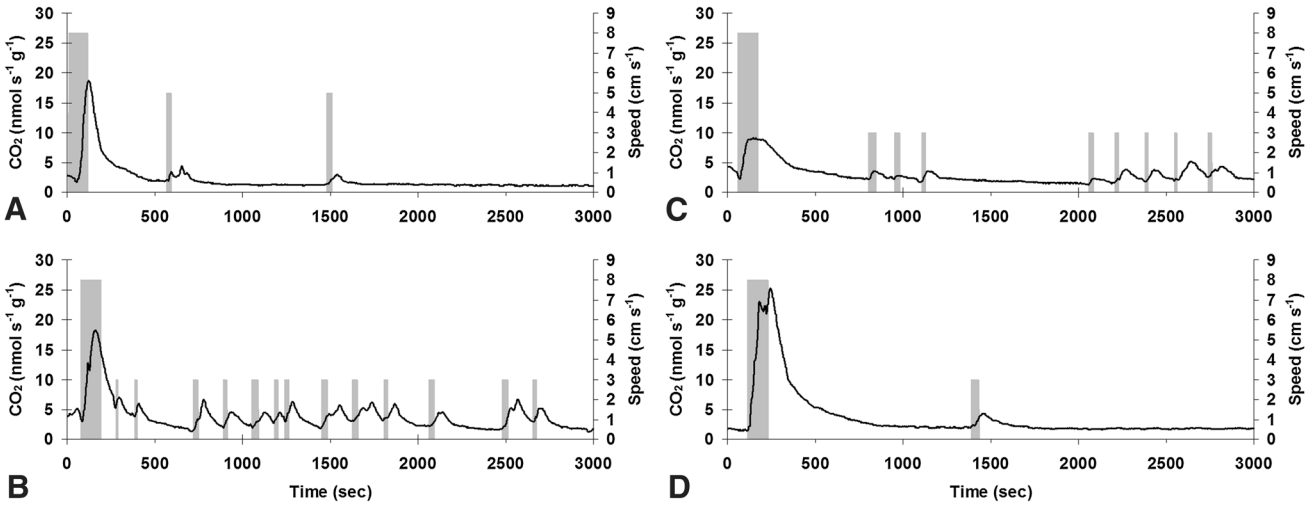

Fig. 3 Maximum CO_2 release of an intact female (**a**, **b**), a female with one lung spiracle sealed (**c**) and an intact male (**d**). Examples for 120-s stimulations are shown. The *line* corresponds to the *left scale* of the figures, while the *gray bars*, showing time and activity, correspond to the *right scale* (speed). The forced activity during stimulation was artificially set to 8 cm s^{-1} (*first bar*) and the other activity periods were set to 5 or 3 cm s^{-1}. In **b** the female had its maximum CO_2 release during activity but was active during the half-time recovery phase. The female with the sealed spiracle (**c**) had a reduced maximum CO_2 release and the male (**d**) had a higher maximum CO_2 release than the females

Miyashita 1969; Seymour and Vinegar 1973; Shillington and Peterson 2002; Watson and Lighton 1994). Feeding, starvation and spontaneous activity resulted in factorial scopes of 4–7 in wolf spiders, tarantulas and in *Nephila* (Jensen et al. 2010; Kasumovic and Seebacher 2013; Nespolo et al. 2011; Tanaka and Itô 1982).

As we measured our spiders without any influence of other spiders or prey, the resting metabolic rates will be real resting values. In the Australian redback spider (*Latrodectus hasselti*, Theridiidae), resting metabolic rate was stated to be lowest if animals were not influenced by conspecifics (Stoltz et al. 2012). Moreover, the resting rate in spiders can be influenced by the life-style, e.g., the cribellum can increase the resting rate, as it was shown for the cribellate spider *Metazygia rogenhoferi* (Araneidae) and the ecribellate *Zosis geniculata* (Uloboridae) (Kawamoto et al. 2011). For crab spiders (Thomisidae), resting rates of 1.75–2.3 nmol s^{-1} g^{-1} O_2 release were measured

Table 5 Comparison of some features of the morphology of lungs and the CO_2 release between *P. phalangioides* and representatives of wolf and jumping spiders

	P. phalangioides	*Pardosa lugubris* (Lycosiade)	*Salticus scenicus* and *Marpissa muscosa* (Salticiade)
Morphology of the lungs			
Barrier thickness (τ), cuticle and epidermis (μm)	0.165	0.17	0.19
Surface areas × body mass^{-1} (cm^2g^{-1})	8	10	9–11
Lung volume × body mass^{-1} ($\times 10^{-6}$ cm^3 mg^{-1})	2.1–2.5	2.3–2.9	2.6–3.6
Diffusing capacity D_{O2} (nmol s^{-1} g^{-1} kPa^{-1})	9	10	9-12
Physiology (CO_2 release and half-time recovery)			
Resting rate (nmol s^{-1} g^{-1})	1.5–1.7	1.7–1.8	1.4–1.5
Maximum spontaneous activity rate (nmol s^{-1} g^{-1})	6	9	11
Maximum rate after stimulation (nmol s^{-1} g^{-1})	17–20	27	29–51
Time to half-recovery (s)	103–140	160-175	95–180

Data from (Schmitz 2004; Schmitz and Perry 2001, 2002)

(Schmalhofer 2011). As these animals were starved, the lower metabolic rates compared with *P. phalangioides* result presumably from starvation.

In the present study, the same methods as in former studies by the same authors were used (Schmitz 2004; Schmitz and Perry 2000, 2001, 2002). Therefore, all data can be well compared. This is necessary to test some hypotheses for the cellar spider: (1) *P. phalangioides* has a lower aerobic capacity than wolf and jumping spiders, (2) the lungs have about the same diffusing capacity as in wolf and jumping spiders, (3) resting metabolic rates do not differ between species of different spider families, (4) resting rates and activity rates do differ between sexes (intraspecific comparison), (5) elimination of one spiracle does not influence the resting rates but halves the maximum activity rates.

Looking at hypothesis one and two, it became clear that aerobic capacities are lower than in wolf and jumping spiders. This might be due to the additional equipment with tracheae and a slightly higher diffusing capacity of the lungs (Table 5) in wolf and jumping spiders. The differing diffusing capacity is mainly due to a bigger surface area, as the barrier thickness might be even slightly higher in wolf and jumping spiders (Table 5). Looking at the metabolic rates (Table 5), jumping spiders have maximum rates of CO_2 release that are 30–150 % higher than in *P. phalangioides*. This is higher, then the lungs could manage as the diffusing capacity for O_2 of the lungs is only up to 30 % higher than in *P. phalangioides* (Table 5). Even if one considers the different body masses of jumping spiders (27–39 mg), wolf spiders (22 mg) and cellar spiders (Table 4), jumping spiders with a well-developed tracheal system have the highest metabolic rates. But tracheae might deliver oxygen not especially to the muscles responsible for movements; however, they might be responsible for higher metabolic rates caused by the eyes during movements (Schmitz 2005).

Prestwich compared a wolf spider, *Lycosa lenta*, and a jumping spider, *Phidippus audax*, and in addition a filistatid spider (*Filistata hibernalis*), which has only rudimentary tracheae (Prestwich 1983b). Animals were stimulated to activity for 120 s by shaking the experimental chamber in combination with glass beads. Aerobic scopes, maximum respiratory rates and also the increase during exercise were greatest in *P. audax* and least in *F. hibernalis*. In addition, recovery periods were shortest in *P. audax*. Prestwich calculated that *P. audax* derives 55 %, *L. lenta* 65 % and *F. hibernalis* 90 % of its power from lactate production (Prestwich 1983a, b, 1988). The jumping spider with the well-developed tracheal system is, therefore, also the most aerobic spider.

According to hypothesis three, resting rates are about the same in all species, but spontaneous activity rates are lower in *P. phalangioides*. This might be the result of higher activity of wolf and jumping spiders (more actively foraging compared with a more sit-and-wait strategy in *P. phalangioides*) and not the result of the morphology of the respiratory organs. Moreover, looking at hypothesis four, no clear pattern in male–female comparison of resting metabolic rates has been demonstrated in other spiders (Humphreys 1977; Kotiaho 1998; Watson and Lighton 1994). In *Pardosa astrigera* and in *P. milvina* (Lycosidae), species without sexual dimorphism, males had higher resting rates than females (Tanaka and Itô 1982; Walker and Irwin 2006). This difference was eliminated by starvation (Tanaka and Itô 1982). In other lycosid species, with a strong sexual dimorphism, mass-specific resting rates did not differ between sexes (Walker and Irwin 2006). In many species, females maintain a larger body size over a longer life span than do males and also have higher energetic costs associated with gamete production (Foelix 1992). Moreover, in the tarantula *Aphonopelma anax* (Theraphosidae) males have higher resting metabolic rates than females

because of their higher needs for their locomotory search for females during the mating season (Shillington 2005). In *P. phalangioides*, males have a slightly higher metabolic rate during rest and after the 120-s stimulation. Resting rates are presumably higher because of the lower body mass (sexual dimorphism) and, therefore, a higher relation of lungs to body mass in males. As females of *P. phalangioides* did not produce eggs during the experiments, the difference in metabolism during activity might be mainly due to a higher activity of the males, but could be the result of the lower average body mass of the males only.

Looking at hypothesis 5, elimination of 1 lung reduces the aerobic metabolism to about the half of an intact animal and, in addition, there was a threefold magnification of the time to half-recovery (Table 4). Even if both lungs send vessels into the opisthosomal heart, elimination of one lung will decrease the oxygen uptake capacity by half. In addition, the maximum CO_2 release in *P. phalangioides* often started already during the stimulation time. This decreased the time to half-recovery in these spiders in comparison with other spider families in which this feature was not observed. Great individual variability in maximum CO_2 release is quite normal and was also shown for other spider species (Anderson and Prestwich 1985; McQueen et al. 1979; Paul and Fincke 1989; Schmitz 2004; Shillington and Peterson 2002).

The oxygen-diffusing capacity (D_{O_2}) has been used as an indicator of the efficiency of respiratory organs. Assuming a respiratory quotient of 0.7, a ΔP_{O_2} of 3 kPa in both sexes would be necessary to support the maximum metabolic rate in *P. phalangioides*. In *Grammostola rosea*, the ΔP_{O_2} was determined to be 0.12–0.16 kPa, which is mainly due to a very high oxygen diffusing capacity of the lungs because of a thin lung epithelium of 0.14 µm (Canals et al. 2007). The physiologically measured ΔP_{O_2} across the lungs of *P. phalangioides* is not known, but for the tarantula *Eurypelma californicum*, a ΔP_{O_2} of 7 kPa was measured after activity (Angersbach 1978). With 3.0 kPa, lungs would, therefore, be not at the limit of their efficiency. As in *P. lugubris* (3.9 kPa) and in *M. muscosa* (4.7–8.1 kPa) (Schmitz 2004), higher values were calculated; these species seem to be more at their limit using the lungs alone as *P. phalangioides*. This is another hint that tracheae in spiders support higher metabolic rates, even if this is the case only in special living situations (Schmitz 2005).

Conclusions

The results of the present study support the hypothesis that tracheae in spiders serve to support higher metabolic rates. Even if this is only for special organ-specific metabolic demands, e.g., visual capabilities in jumping spiders (Foelix 1992; Schmitz 2005; Schmitz and Perry 2001) or net constructing in Uloboridae (Opell 1987), tracheae increase the D_{O_2} of the entire respiratory system. The function of the circulatory system was not considered in the present study, but could also play an important role in aerobic capabilities of spiders.

Acknowledgments I am indebted to Prof. Dr. S.F. Perry who made these experiments possible.

References

Anderson JF (1970) Metabolic rates in spiders. Comp Biochem Physiol 33:51–72

Anderson JF, Prestwich KN (1985) The physiology of exercise at and above maximal aerobic capacity in a theraphosid (tarantula) spider, *Brachypelma smithi*. J Comp Physiol B 155:529–539

Angersbach D (1978) Oxygen transport in the blood of the tarantula *Eurypelma californicum*: pO2 and pH during rest, activity and recovery. J Comp Physiol 123:113–125

Baddeley AJ, Gundersen HJG, Cruz-Orive LM (1986) Estimation of surface area from vertical sections J. Microscopy 142(3):259–276

Bartels H (1971) Diffusion coefficients and Krogh's diffusion constants. In: Altman PL, Dittmer DS (eds) Respiration and Circulation. Biological Handbooks. Federation of American Societies for Experimental Biology, Bethesda, pp 21–22

Canals M, Salazar MJ, Duran C, Figueroa D, Veloso C (2007) Respiratory refinements in the mygalomorph spider *Grammostola rosea walckenaer* 1837 (Araneae, Theraphosidae). J Arachnol 35:481–486

Cruz-Orive LM (1993) Systematic sampling in stereology. Bull Int Statistic Inst Proc 49:451–468

Culik BM, McQueen DJ (1985) Monitoring respiration and activity in the spider Geolycosa domifex (Hancock) using time-lapse television and CO_2-analysis. Can J Zool 63:843–846

Foelix RF (1992) Biologie der Spinnen, 2nd edn. Georg Thieme Verlag, Stuttgart

Ford MJ (1977a) Energy costs of the predation strategy of the web-spinning spider *Lethyphantes zimmermanni* Bertkau (Linyphiidae). Oecologica 28:341–349

Ford MJ (1977b) Metabolic costs of the predation strategy of the spider *Pardosa amentata* (Clerck) (Lycosidae). Oecologica 28:333–340

Gundersen HJG, Jensen EB (1987) The efficiency of systematic sampling in stereology and its prediction J. Microscopy 147:229–263

Howard CV, Reed MG (1998) Unbiased stereology. Three-dimensional measurement in micrsocopy. BIOS Scientific Publishers, Oxford

Humphreys WF (1977) Respiration studies on *Geolycosa godeffroyi* (Aranea: Lycosidae) and their relationship to field estimates of metabolic heat loss. Comp Biochem Physiol 57A:255–263

Jensen K, Mayntz D, Wang T, Simpson SJ, Overgaard J (2010) Metabolic consequences of feeding and fasting on nutritionally different diets in the wolf spider Pardosa prativaga. J Insect Physiol 56:1095–1100. doi:10.1016/j.jinsphys.2010.03.001

Kasumovic MM, Seebacher F (2013) The active metabolic rate predicts a male spider's proximity to females and expected fitness. Biol Lett 9:20121164. doi:10.1098/rsbl.2012.1164

Kawamoto TH, Machado FdA, Kaneto GE, Japyassu HF (2011) Resting metabolic rates of two orbweb spiders: a first approach to evolutionary success of ecribellate spiders. J Insect Physiol 57:427–432. doi:10.1016/j.jinsphys.2011.01.001

Kotiaho J (1998) Sexual differences in metabolic rates of spiders. J Arachnol 26:401–404
Krogh A (1919) The rate of diffusion of gases through animal tissues, with some remarks on the coefficient of invasion. J Physiol 52:391–408
Levi HW (1976) On the evolution of tracheae in Arachnids. Bull Br Arachnol Soc 3(7):187–188
McQueen DJ (1980) Active respiration rates for the burrowing wolf spider Geolycosa domifex (Hancock). Can J Zool 58:1066–1074
McQueen DJ, Culik B (1981) Field and laboratory activity patterns in the burrowing wolf spider *Geolycosa domifex* (Hancock). Can J Zool 59:1263–1271
McQueen DJ, Jensen IM, Dyer BS (1979) Resting and diel respiration rates for burrowing wolf spider *Geolycosa domifex* (Hancock). Can J Zool 57:1922–1933
Michel RP, Cruz-Orive LM (1988) Application of the cavalieri principle and vertical sections method to lung: estimation of volume and pleural surface area. J Microsc 150:117–136
Miyashita K (1969) Effects of locomotory activity, temperature and hunger on the respiratory rate of Lycosa t-insignita Boes et. Str. (Araneae: Lycosidae). Appl Ent Zool 4:105–113
Nespolo RF, Correa L, Perez-Apablaza CX, Cortes P, Bartheld JL (2011) Energy metabolism and the postprandial response of the Chilean tarantulas, *Euathlus truculentus* (Araneae: Theraphosidae). Comp Biochem Physiol A-Mol Integr Physiol 159:379–382. doi:10.1016/j.cbpa.2011.04.003
Opell BD (1987) The influence of web monitoring tactics on the tracheal systems of spiders in the family Uloboridae (Arachnida, Araneida). Zoomorphology 107:255–259
Packard GC, Boardman TJ (1988) The misuse of ratios, indices, and percentages in ecophysiological research. Physiol Zool 61:1–9
Paul R, Fincke T (1989) Book lung function in arachnids II. Carbon dioxide and its relations to respiratory surface, water loss and heart frequency. J Comp Physiol 159:419–432
Paul RJ, Bihlmayer S, Colmorgen M, Zahler S (1994) The open circulatory system of spiders (*Eurypelma californicum*, *Pholcus phalangioides*): a survey of functional morphology and physiology. Physiol Zool 67(6):1360–1382
Perry SF (1978) Quantitative anatomy of the lungs of th ered-eared turtle, Pseudemys scripta elegans. Resp Physiol 35:245–262
Perry SF (1981) Morphometric analysis of pulmonary structure: methods for evaluation and comparison of unicameral lungs. Mikroskopie 38:278–293
Perry SF, Hein J, van Dieken E (1994) Gas exchange morphometry of the lungs of the tokay, *Gekko gecko* (Squamata). J Comp Physiol B 164:206–214
Prestwich KN (1983a) Anaerobic metabolism in spiders. Physiol Zool 56(1):112–121
Prestwich KN (1983b) The roles of aerobic and anaerobic metabolism in active spiders. Physiol Zool 56(1):122–132
Prestwich KN (1988) The constraints on maximal activity in spiders. I. Evidence against the fluid insufficiency hypothesis. J Comp Physiol 158:437–447
Schmalhofer VR (2011) Impacts of temperature, hunger and reproductive condition on metabolic rates of flower-dwelling crab spiders (Araneae: Thomisidae). J Arachnol 39:41–52
Schmitz A (2004) Metabolic rates during rest and activity in differently tracheated spiders (Arachnida, Araneae): *Pardosa lugubris* (Lycosidae) and *Marpissa muscosa* (Salticidae). J Comp Physiol B 174:519–526
Schmitz A (2005) Spiders on a treadmill: influence of running activity on metabolic rates in *Pardosa lugubris* (Araneae, Lycosidae) and *Marpissa muscosa* (Araneae, Salticidae). J Exp Biol 208:1401–1411
Schmitz A (2013) Tracheae in spiders: Respiratory organs for special functions. In: Nentwig W (ed) Spider Ecophysiology. Springer, New York, pp 29–39
Schmitz A, Perry SF (2000) Respiratory system of arachnids I: morphology of the respiratory system of Salticus scenicus and *Euophrys lanigera* (Arachnida, Araneae, Salticidae). Arthropod Struct Dev 29:3–12
Schmitz A, Perry SF (2001) Bimodal breathing in jumping spiders: morphometric partitioning of lungs and tracheae in *Salticus scenicus* (Arachnida, Araneae, Salticidae). J Exp Biol 204:4321–4334
Schmitz A, Perry SF (2002) Respiratory organs in wolf spiders: morphometric analysis of lungs and tracheae in *Pardosa lugubris* (L.) (Arachnida, Araneae, Lycosidae). Arthropod Struct Dev 31:217–230
Seymour RS, Vinegar A (1973) Thermal relations, water loss and oxygen consumption of a north american tarantula. Comp Biochem Physiol 44A:83–96
Shillington C (2005) Inter-sexual differences in resting metabolic rates in the Texas tarantula. Aphonopelma anax Comp Biochem Physiol A-Mol Integr Physiol 142:439–445
Shillington C, Peterson CC (2002) Energy metabolism of male and female tarantulas (*Aphonopelma anax*) during locomotion. J Exp Biol 205:2909–2914
Stoltz JA, Andrade MCB, Kasumovic MM (2012) Developmental plasticity in metabolic rates reinforces morphological plasticity in response to social cues of sexual selection. J Insect Physiol 58:985–990. doi:10.1016/j.jinsphys.2012.05.002
Strazny F, Perry SF (1987) Respiratory system: structure and function. In: Nentwig W (ed) Ecophysiology of spiders. Springer, Berlin, pp 78–94
Tanaka K, Itô Y (1982) Decrease in respiratory rate in a wolf spider, *Pardosa astrigera* (L. Koch), under starvation. Res Popul Ecol 24:360–374
Walker SE, Irwin JT (2006) Sexual dimorphism in the metabolic rate of two species of wolf spider (Araneae, Lycosidae). J Arachnol 34:368–373
Watson PJ, Lighton JRB (1994) Sexual selection and the energetics of copulatory courtship in the Sierra dome spider. Linyphia litigiosa Anim Behav 48:615–626
Weibel ER (1970/1971) Morphometric estimation of pulmonary diffusion capacity. Resp Physiol 11:54–75
Weibel ER, Knight BW (1964) A morphometric study on the thickness of the pulmonary air-blood barrier. J Cell Biol 21:367–384
Withers PC (1977) Measurement of V_{O2}, V_{CO2}, and evaporative water loss with a flow-through mask. J Appl Physiol 42:120–123